

Supporting Information

Chemical Structure, Ensemble and Single Particle Spectroscopy of Thick-Shell InP-ZnSe Quantum Dots

Kemar R. Reid^{1,2}, James R. McBride^{*2,3}, Nathaniel J. Freymeyer^{2,3}, Lucas B. Thal³, Sandra J. Rosenthal^{*1-5}

¹Department of Interdisciplinary Materials Science, ²Vanderbilt Institute for Nanoscale Science and Engineering, ³Department of Chemistry, ⁴Department of Physics and Astronomy, ⁵Department of Pharmacology, Chemical and Biomolecular Engineering, Vanderbilt University, Nashville, Tennessee 37235, United States

* Email correspondence: james.r.mcbride@vanderbilt.edu, sandra.j.rosenthal@vanderbilt.edu

Materials

Indium (III) acetate (99.99%-in), tris(trimethylsilyl)phosphine (95%), myristic acid (99%), oleic acid (90%, technical grade), 1-octadecene (ODE, 90%, technical grade), trioctylamine (TOA, 98%) and trioctylphosphine (TOP, 97%) were obtained from Aldrich. Zinc acetate (98%, extra pure) was obtained from Acros Organics. Selenium powder (99.99%, 200 mesh) was obtained from Alfa Aesar. Sulfur powder (99.99%), isopropanol (99.9%) and toluene (99.9%) were obtained from Fisher Scientific. All chemicals were used without further purification unless noted otherwise.

Precursor preparation

- Indium myristate and zinc myristate were synthesized according to a previously published method¹.

- Zinc oleate (0.4 M) was prepared by heating 1.6 g of zinc acetate in 12 mL of oleic acid and 8 mL TOP under argon at 150 °C for 30 min until the zinc acetate was dissolved. The solution was then degassed at 100 °C under vacuum for 30 min.
- TOP-Se (0.4 M) was prepared by dissolving 640 mg of selenium powder in 20 mL TOP with stirring overnight in a nitrogen-filled drybox.
- TOP-S (0.4 M) was prepared by heating 256 mg of sulfur in 20 mL TOP at 100 °C until completely dissolved in a nitrogen drybox.

InP core synthesis

InP QD cores were synthesized using a modified literature protocol². Briefly, 160 mg (0.2 mmol) indium myristate and 5 mL ODE were added to a 100 mL three-neck round-bottom flask. The mixture was heated to 100 °C with stirring and degassed under vacuum for 30 min. The reaction was then placed under an argon atmosphere and heated to 300 °C. In a nitrogen drybox, 45 μ L (0.15 mmol) tris(trimethylsilyl)phosphine ((TMS)₃P) was mixed with 1 mL TOP. The (TMS)₃P solution was quickly injected into the reaction flask and the QDs grown for 30 minutes before cooling to room temperature. The nanocrystals obtained were typically 3 nm in diameter.

ZnSe and ZnS shell growth

For ZnSe shell growth, 50 mg of zinc myristate and 3 mL TOA were loaded into the reaction flask consisting of freshly made InP cores. The mixture was degassed at 100 °C under vacuum for 30 min to remove water and oxygen inside the solution. The flask was then filled with argon and heated to 300 °C. A mixture of zinc oleate (6 mL, 0.4 M stock) and

TOP-Se (6 mL, 0.4 M stock) was added drop-wise into the growth solution at a rate of 1.5 mL/h using a syringe pump. The reaction solution was further annealed at 300 °C for 2 h. After cooling to room temperature the crude InP-ZnSe core-shell stock was stored in a nitrogen drybox. Samples for optical and structural characterization were prepared by washing with isopropanol and re-dispersing in toluene twice. ZnS shell growth was carried out using the above procedure, substituting TOP-S for TOP-Se.

Transmission electron microscopy (TEM) imaging

HRTEM, SAED, HRSTEM images were obtained using a Tecnai Osiris TEM/STEM operating at 200 kV equipped with a SuperX™ quad EDS detection system. Samples were baked at 165 °C under high vacuum prior to imaging. STEM-EDS maps were acquired using the Bruker Esprit software with a sub-nm probe having ~ 1 nA of beam current (Spot size 6). Quantification was performed using the Cliff Lorimer method. Nanocrystal sizes were determined by manually measuring the diameters of QDs from TEM images in the ImageJ software.

Powder X-ray diffraction

Powder X-ray diffraction (XRD) measurements were obtained using a Rigaku SmartLab X-Ray diffractometer operating at 40 kV and 44 mA using a Cu K α line (λ = 1.5418 angstrom). XRD patterns were collected at a scan rate of 2 deg/min.

Ensemble spectroscopy

Absorption spectra were recorded on a Cary 60 UV-VIS spectrometer. Photoluminescence (PL) spectra were collected on a PTI QuantaMaster fluorescence spectrophotometer using a 75 W Xe arc lamp as the excitation source. PL was measured with a 1 sec. integration time and a 1 nm slit width. Quantum Yield (QY) measurements were determined by comparing the PL of the QDs to a reference dye (R6G in methanol, QY ~ 94%).

Time-resolved photoluminescence (TRPL) measurements were performed on dilute solutions of QDs with optical densities below 0.2 at the lowest-energy absorption transition. The QD solutions were excited under wide-field illumination using a 400 nm pulsed source (200 fs pulse duration) at a 250 KHz repetition rate. PL from the solutions was filtered with an appropriate long-pass filter and directed onto a single-photon avalanche photo-diode (SPAD, Micro Photon Devices, PD-050-0TC). A time-correlated single photon-counting unit (TCSPC, PicoHarp 300, $\Delta t_{res} \sim 35$ ps) was used to generate a histogram of photon arrival times. Ensemble lifetimes were determined by fitting the histogram of arrival times to a tri-exponential function:

$$I_{PL}(t) = \sum_i A_i \exp(-t/\tau_i) \quad (1)$$

The average lifetime, τ_{avg} was calculated using the fit components as follows:

$$\tau_{avg} = \frac{\sum_i^n A_i \tau_i}{\sum_i^n A_i} \quad (2)$$

For multi-exciton decay measurements, TRPL decay traces were normalized at long delay times, corresponding to single-exciton recombination. Low pump-fluence decay curves

were subtracted from decay profiles acquired at high pump-fluences to extract the multi-exciton contribution to the decay. The extracted decay profiles were fit to single exponential decays.

Single QD PL blinking measurement

For single nanocrystal blinking measurements, core-shell QDs were diluted to ~ 1 nM concentration in toluene and drop-cast onto a No. 0 glass cover-slip. The resulting dried QD films were then packaged between the cover-slip and a cover glass and the assembly sealed with epoxy. The entire sample preparation was carried out in a nitrogen dry-box in order to minimize the influence of photo-oxidative degradation on the blinking behavior of the QDs over the time period investigated. Room temperature single QD intensity-time traces were acquired in wide-field configuration of a custom-built epi-fluorescence microscope³. The microscope uses a water immersion objective (Olympus, 60X, 1.2 NA). QDs were excited by a 400 nm, 76 MHz laser focused to a spot ~ 60 μm in diameter. The average excitation power density was $\sim 5 W/cm^2$. Emission from individual dots was collected through the objective and imaged onto an EM-CCD camera (Andor, iXonEM+, DU-897e-CSO-#BV). Intensity-time traces were recorded at 10 Hz (100 ms per frame).

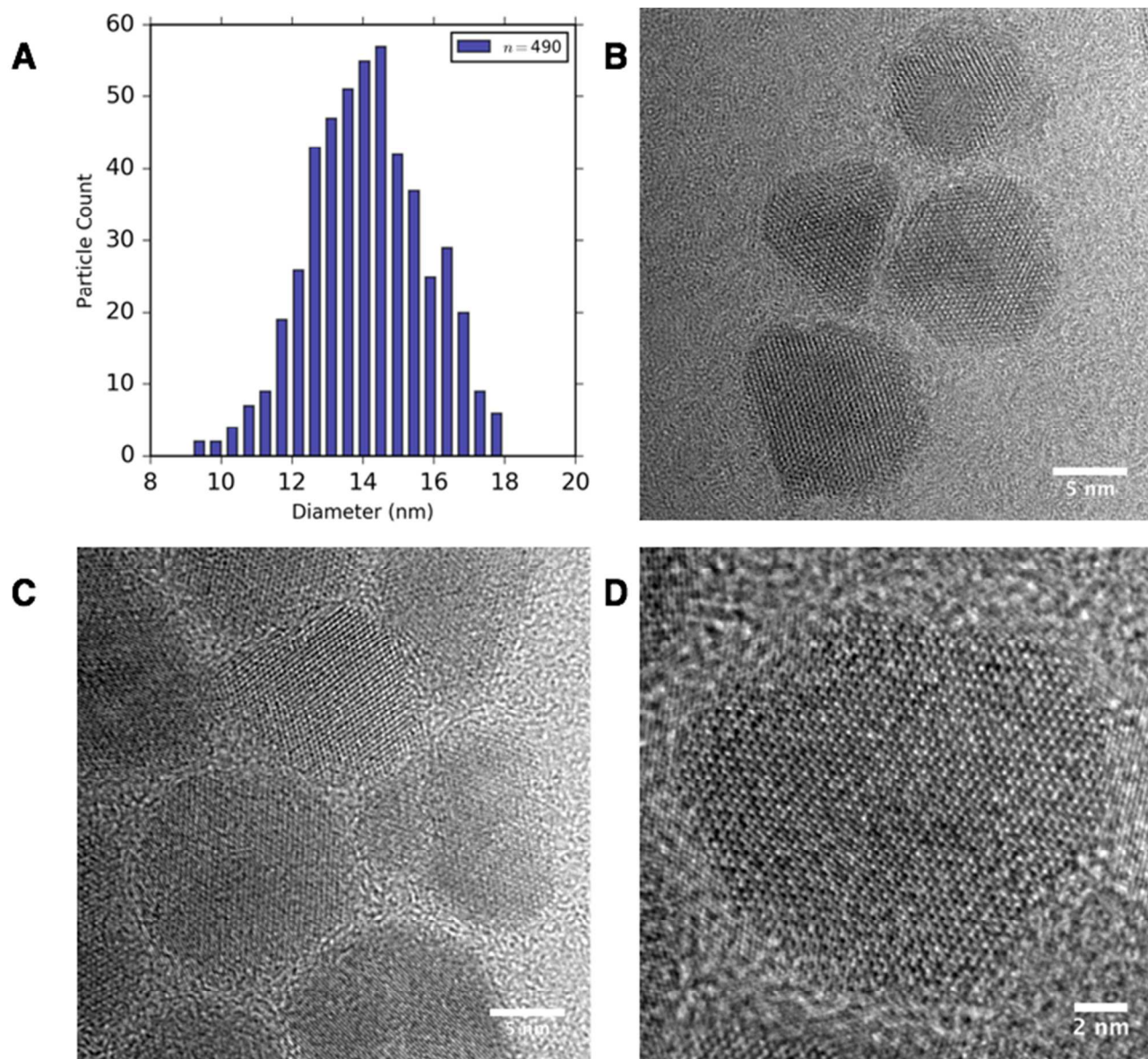


Figure S1. (a) Size distribution and (b-d) additional high resolution TEM images of the thick-shell InP-ZnSe QDs. The average particle diameter is $\sim 14.1 \pm 1.6$ nm

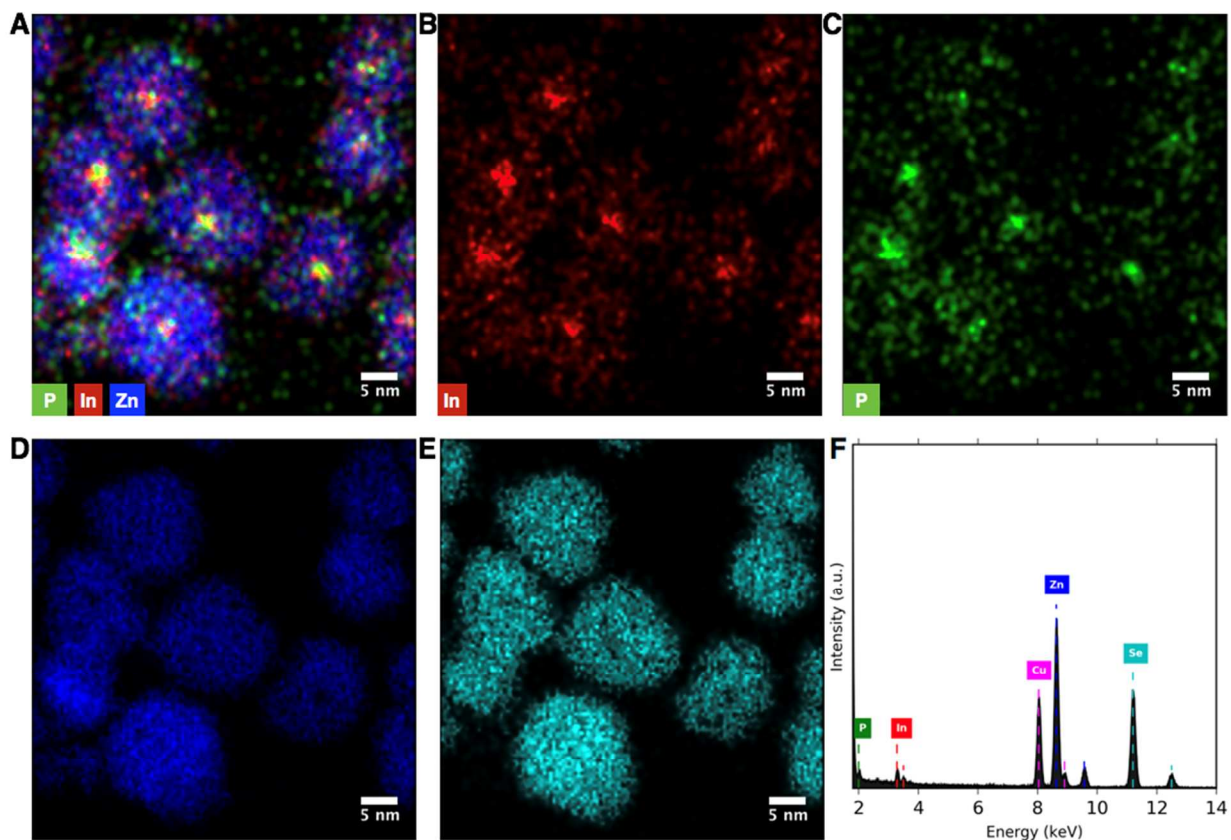


Figure S2. Elemental characterization of thick-shell InP-ZnSe QDs. Energy dispersive X-ray (EDX) chemical map of several core-shell InP-ZnSe QD. (b) Indium, (c) Phosphorus, (d) Zinc and (e) Selenium chemical maps from the particles in a. (f) EDX spectra of the thick-shell InP-ZnSe QDs. Relative atomic percentages: In - 2.2% , P - 1.8% , Zn - 50% , Se - 46%.

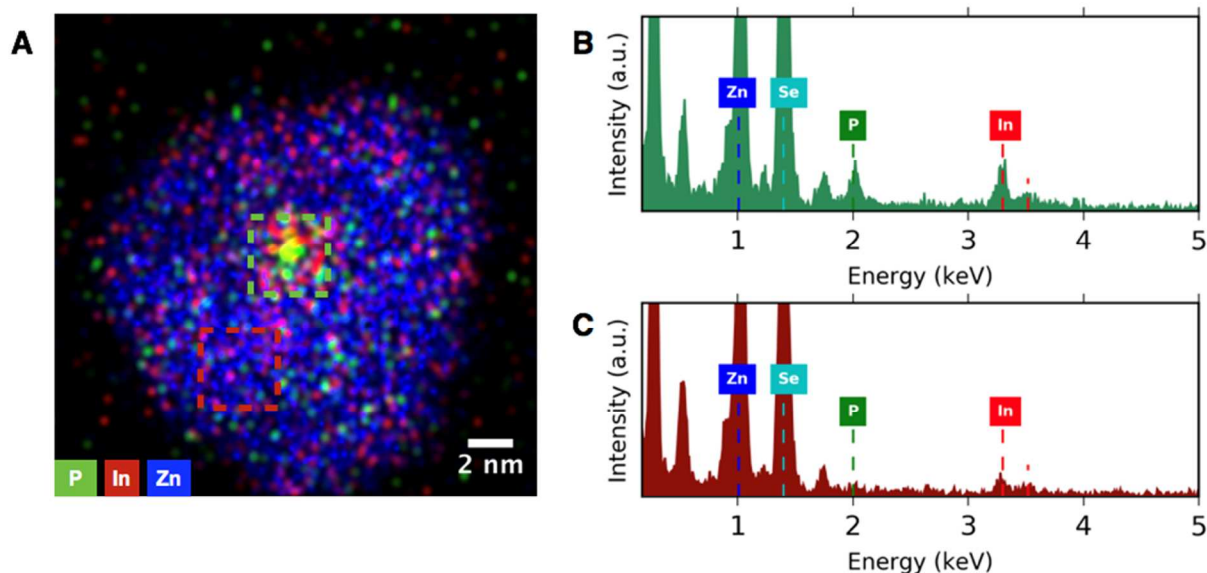


Figure S3. Quantification of Indium in the thick-shell InP-ZnSe QDs. (a) Energy dispersive X-ray (EDX) map of the thick-shell InP-ZnSe QD in figure 2a. The region of interests (ROIs) labeled in green and red correspond to core and shell regions respectively of the core-shell particle. (b) EDX spectra for the core ROI. (c) EDX spectra rendered from the shell ROI. Average atomic percentages of In: core ROI (4.8%), shell ROI (2.3%) ($n=7$). Average atomic percentages of P: core ROI (4.1%), shell ROI (undetected) ($n=7$).

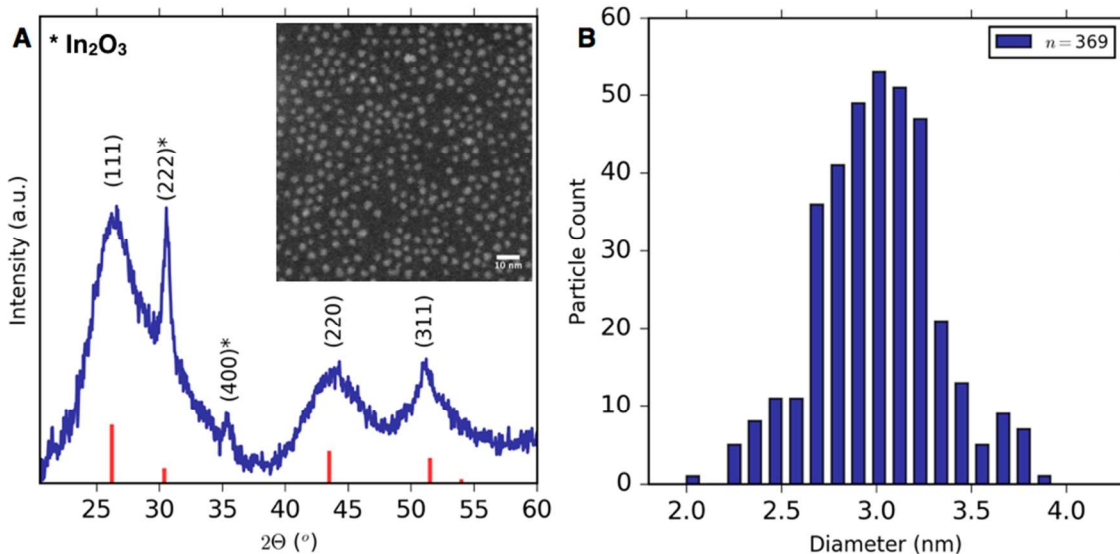


Figure S4. (a) X-ray powder diffraction pattern obtained from the InP starting cores. The stick pattern (red) shows the reference peaks of bulk zinc blende InP. Peaks resulting from oxidation to In_2O_3 are denoted by an asterisk (*). Inset: HAADF-STEM image of the particles. (b) Size distribution of the InP cores. The average particle diameter is $\sim 3.0 \pm 0.3$ nm

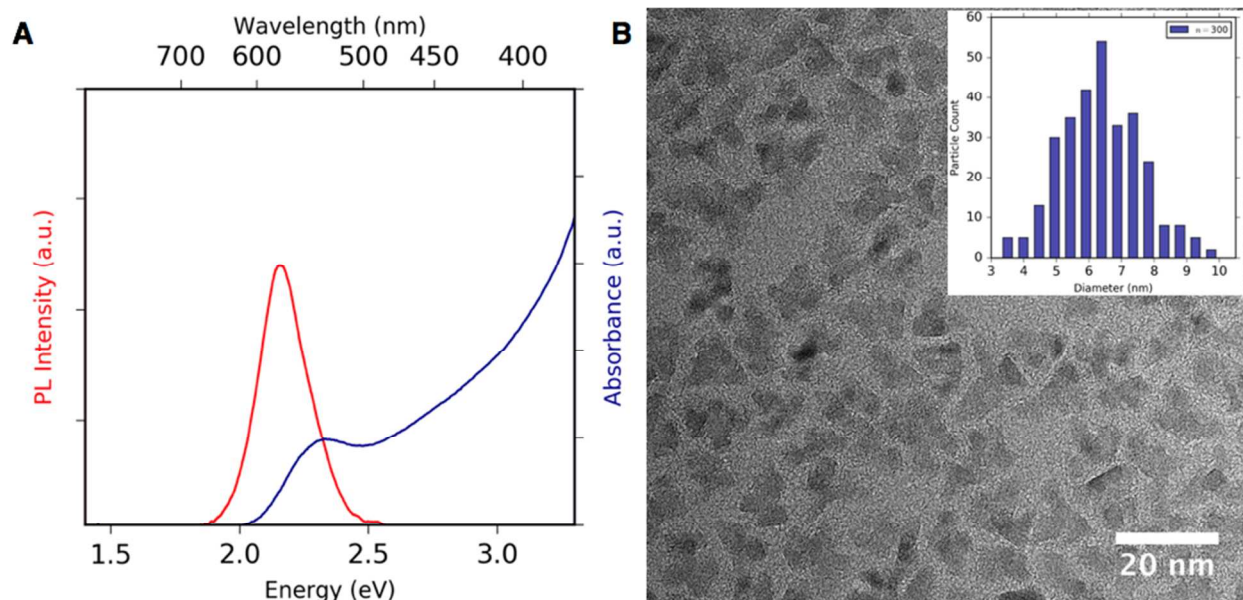


Figure S5. Characterization of InP-ZnS QDs. (a) Absorption (blue) and Photoluminescence (red) spectra of the InP-ZnS QDs. The PL is centered around 585 nm with a FWHM ~ 51 nm (165 meV) and PL QY $\sim 43\%$. (b) The corresponding TEM image of the sample in a. Inset: Size distribution of the InP-ZnS QDs. The average particle diameter is $\sim 6.3 \pm 1.3$ nm. The InP-ZnS QDs produced are highly irregular, have a poor size distribution ($\sim 20\%$) and the average shell thickness (~ 1.7 nm) obtained is significantly less compared to employing ZnSe as the shelling material.

Table S1. PL dynamics fit parameters

QD Sample	τ_1 (ns)	A1	τ_2 (ns)	A2	τ_3 (ns)	A3	τ_{avg} (ns)	τ_{2X} (ps)
InP	1.8	0.6	23.7	0.28	169.4	0.12	28	-
InP-ZnS	23.6	0.5	64.1	0.485	292.4	0.015	47	78 \pm 5
InP-ZnSe	35.4	0.79	119.9	0.175	545	0.035	68	540 \pm 30

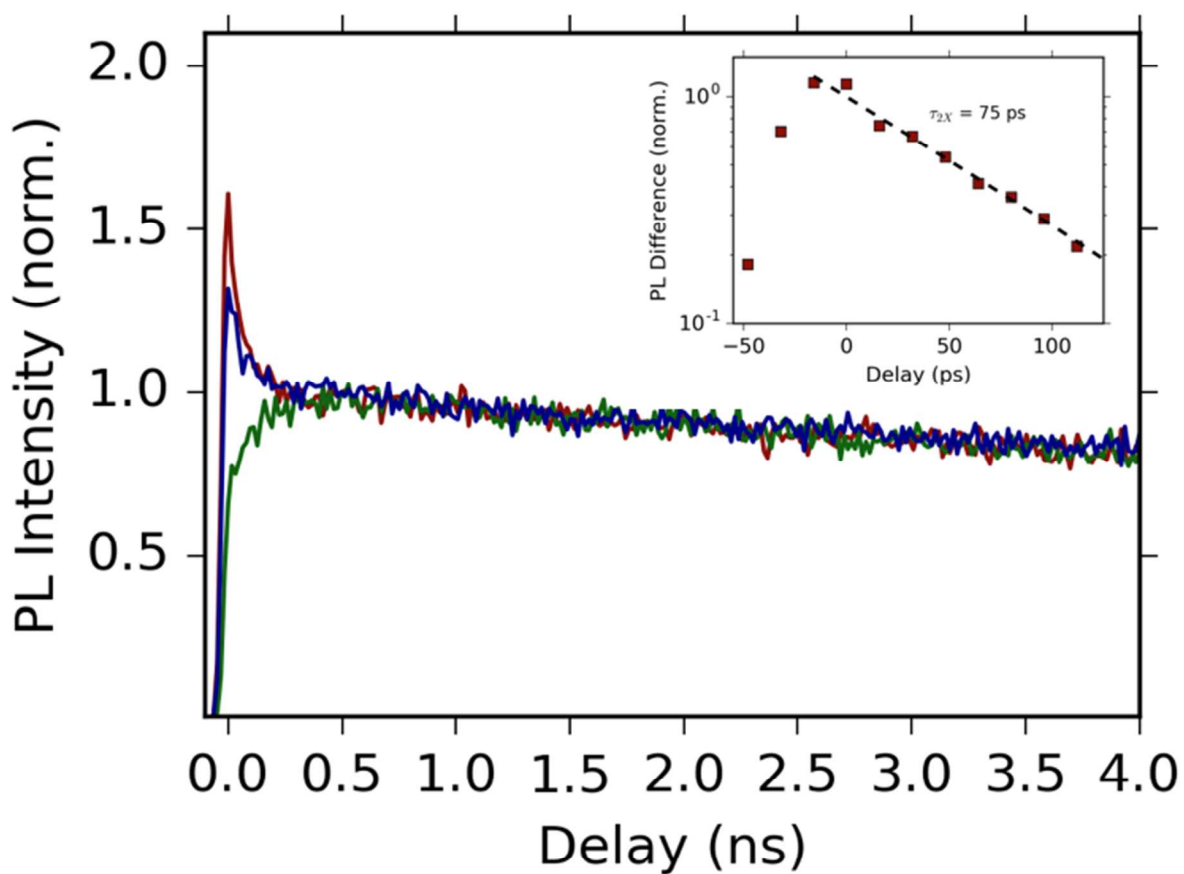


Figure S6. Pump-fluence-dependent PL dynamics of InP-ZnS QDs normalized at long time. The inset shows an example of the extracted multi-exciton decay component fitted to a single-exponential decay (dashed line) with a 75 ± 5 ps bi-exciton lifetime.

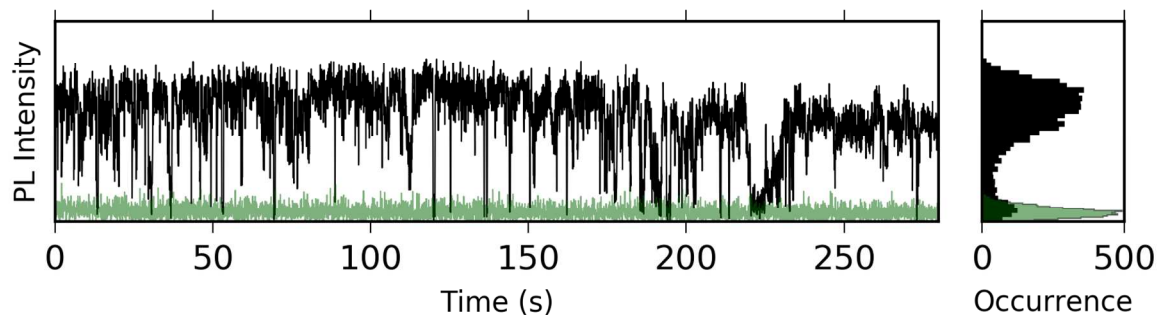


Figure S7. Additional blinking trace and intensity histogram of an individual thick-shell InP-ZnSe QD recorded in air using a lower energy excitation source (488 nm, 2.5 eV). The background (green trace) was recorded from a region with no QDs.

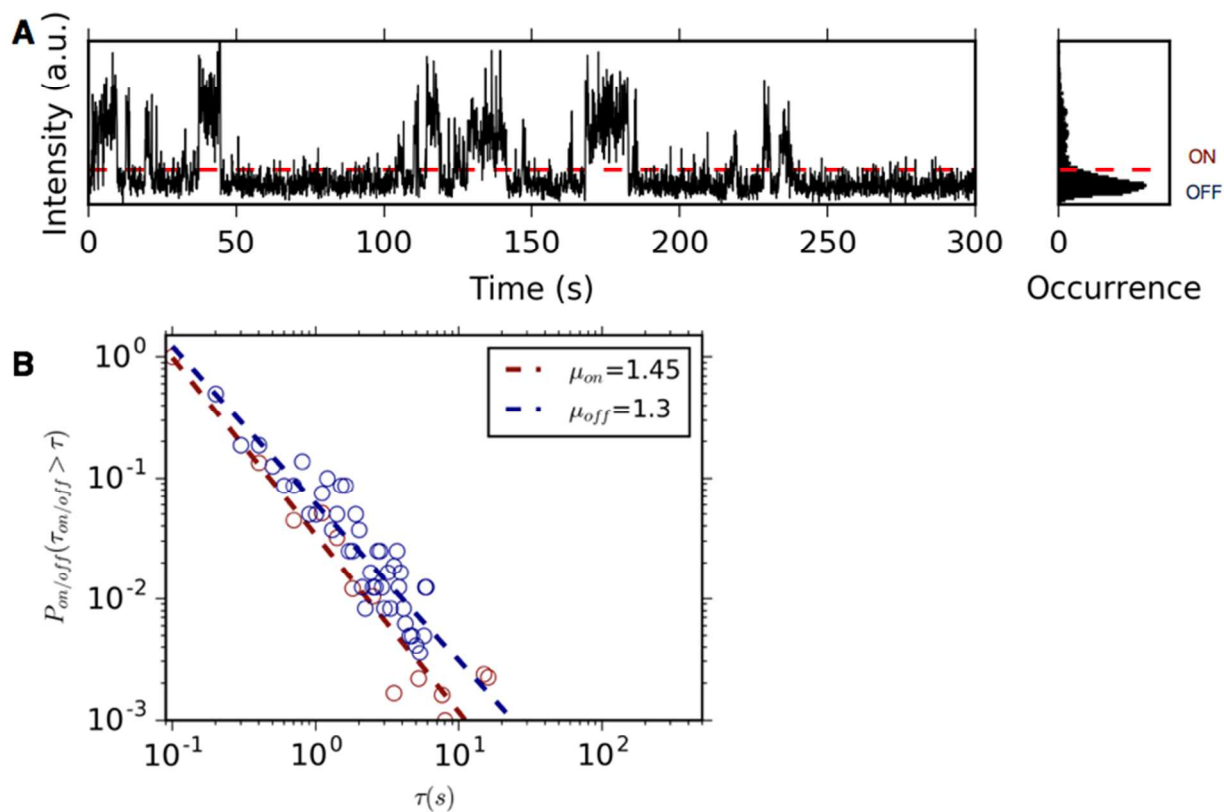


Figure S8. (a) Representative single QD intensity-time trace and intensity distribution from the InP-ZnS sample synthesized by our method for which the extracted ON-time fraction was 20% ($n=15$). The dashed red line represents the chosen ON-OFF threshold. (b) Distribution of ON (red) and OFF (blue) time durations plotted on a log-log scale. Dashed lines represent power-law ($\tau^{-\mu_{off/on}}$) fits to the data, $\mu_{off} = 1.3$ and $\mu_{on} = 1.45$.

References

- (1) Harris, D. K.; Bawendi, M. G. Improved Precursor Chemistry for the Synthesis of III–V Quantum Dots. *J. Am. Chem. Soc.* **2012**, *134*, 20211–20213.
- (2) Gary, D. C.; Cossairt, B. M. Role of Acid in Precursor Conversion During InP Quantum Dot Synthesis. *Chem. Mater.* **2013**, *25*, 2463–2469.
- (3) Orfield, N. J.; McBride, J. R.; Keene, J. D.; Davis, L. M.; Rosenthal, S. J. Correlation of Atomic Structure and Photoluminescence of the Same Quantum Dot: Pinpointing Surface and Internal Defects That Inhibit Photoluminescence. *ACS Nano* **2015**, *9*, 831–839.